Behavior of monocrystalline silicon under cyclic microindentations with a spherical indenter

I. Zarudi and L. C. Zhang[a)]
School of Aerospace, Mechanical and Mechatronic Engineering, The University of Sydney, NSW 2006, Australia

M. V. Swain
School of Aerospace, Mechanical and Mechatronic Engineering, Biomaterials Science Research Unit, The University of Sydney, Eveleigh, NSW 1430, Australia

(Received 1 July 2002; accepted 6 December 2002)

This study discusses the behavior of high-pressure phases of monocrystalline silicon when subjected to cyclic indentations with a spherical indenter. It was found that specific phases form in the second and subsequent indentation cycles under low maximum loads. An increase of the maximum indentation load causes changes of subsequent indentation cycles of the phase transformation events to occur earlier on both loading and unloading. The repeated indentations result in the formation of a multiphase structure in the deformed zone, featuring a nonhysteresis behavior. After a critical stage, the properties of the transformed material are stabilized and further indentations can no longer alter the load–displacement curve. It was also found that the greater the maximum load, the faster the occurence of property stabilization. © *2003 American Institute of Physics.*
[DOI: 10.1063/1.1541110]

The indentation of silicon and its related microstructural changes have been the focus of research over the last decade.[1–11] It has been understood that in the first indentation cycle, the diamond structure of monocrystalline silicon, or Si-I, undergoes the first phase transformation to the β-Sn phase, or Si-II, on loading,[3,10] followed by the second phase transformation on unloading. The second transformation can be to the amorphous phase or crystalline Si-XII/Si-III (R8/BC8) rhombohedral/body-centered-cubic phases, depending on the specific loading–unloading conditions.[1,3,5,8,12] It was also claimed that with a spherical indenter, the so-called pop-in and pop-out on loading and unloading are related to the phase transformation to the β-Sn and Si-XII/Si-III phases, respectively.[5] These events set off the well-known silicon indentation curves with a substantial hysteresis.[1,5]

The microstructure of the transformed materials after a single indentation cycle has been explored in detail by means of Raman spectroscopy and cross-sectional transmission electron microscopy.[1,8,9] The transformation zones were found to be amorphous, crystalline, or a mixture of crystalline and amorphous phases, depending on the maximum indentation load[1] and the loading/unloading rate[5,12] It was also believed that the phases formed during indentation loading were metastable.[13–15] However, details of their mechanical properties have never been investigated.

It was reported that under repeated indentations with a Berkovich indenter,[16] the load displacement showed nondegenerative hysteresis under low indentation loads. At a higher indentation load, however, the hysteresis disappeared in the second cycle as a result of crack initiation in the subsurface. It was concluded that the nondegenerative hysteresis appears due to phase transformation events in indentation but no further details were presented.

The present study reports the special behavior of monocrystalline silicon identified under cyclic microindentations with a spherical indenter. This type of indenter enables one to detect phase transformation events on loading (pop-in), estimate the stress field induced, and avoid cracking. It, therefore, enables a focus on the effect of phase transformation.

The test material was a monocrystalline silicon (100) wafer. The spherical indenter used had a nominal radius of 5 μm. The indentation tests were conducted on an Ultra-Micro Indentation System-2000. To capture the effect of the magnitude of indentation load, three sets of maximum loads, $P_{\max}=30$ mN, 50 mN, and 90 mN, were tested, respectively. 50 tests were performed for every $P_{\max}$. In each cycle of an indentation, thirty steps were set on both the loading and unloading paths, which gave an average loading/unloading rate of about 0.6 mN/s. In each test with a given $P_{\max}$, five cycles of indentations were carried out. To characterize the stress-induced structures, Raman analysis was completed using a Renishaw Raman Systems 2000 Microprobe with 514.5 nm excitation operated in the confocal mode with a spot size of 1 μm and a depth of focus of 2 μm.

Figure 1 shows the evolution of the load–displacement curves in cyclic indentations. With $P_{\max}=30$ mN [Fig. 1(a)], the curves of the first cycle of the 50 tests show either an elbow (change of slope) during unloading (17 of the curves), indicating in the case of Berkovich indentations a greater likelihood of amorphous phase formation,[8] or an elbow with a small pop-out (33 of the curves), indicating a minor crystalline decomposition along with the major amorphous transformation. The pop-in during loading (marked in Fig. 1) represents a phase transformation from diamond to β-Sn phase according to the relevant theoretical prediction.[4,6] In the second cycle, the slope of the loading curve increased slightly, giving rise to a greater effective Young's modulus, 138 GPa.

a)Electronic mail: zhang@mech.eng.usyd.edu.au

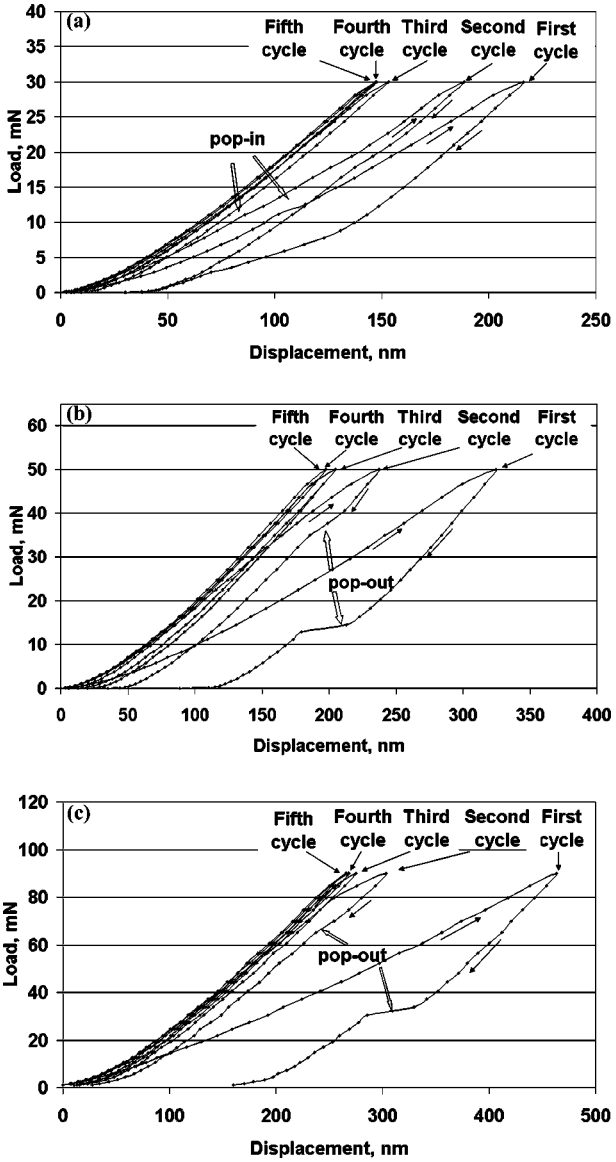

FIG. 1. Load–displacement curves in five indentation cycles with different maximum loads: (a) $P_{max}=30$ mN, (b) $P_{max}=50$ mN, and (c) $P_{max}=90$ mN. Note, that the second and subsequent loading cycles were shifted to zero displacement.

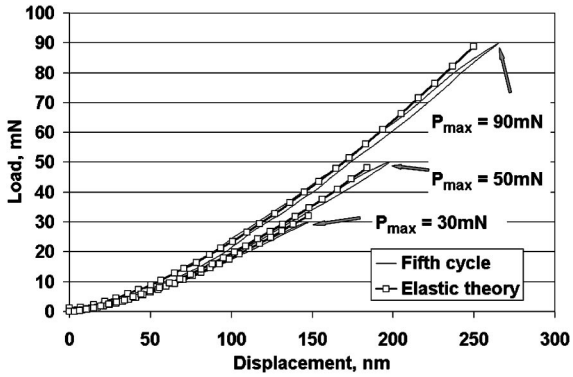

FIG. 2. Comparison of the curves at the fifth indentation cycle with corresponding elastic theory.

Young's modulus were calculated by the method described in Ref. 17. In calculating Young's modulus after the first indentation cycle, the concavity of the residual indentation impression, measured by an atomic force microscope (AFM), was taken into account. With this, the effective radius of the indenter can be calculated using the theory of contact mechanics.[7,17] In this cycle, the pop-in during loading is still noticeable and the unloading curve shows a bend that can be viewed as a gentle pop-out at a much higher portion of the curve if compared with that in the first indentation cycle. It is interesting to note that the material behavior becomes more and more stable upon the repeated indentations. As shown in Fig. 1(a), the load–displacement curves of the fourth and fifth cycles are nearly identical, with almost no hysteresis. It is even more interesting to note that the response of the material in the later cycles becomes nearly elastic, as shown in Fig. 2, where the theoretical curve was based on the elastic indentation theory[17] with the effective Young's modulus $=139$ GPa. Recalling that the effective Young's modulus changes from the original 137 GPa of the diamond-structured silicon, to 138 GPa at the second cycle, to 139 GPa at the fourth cycle and to a constant, it seems reasonable to conclude that there exists a gradual complete phase transformation process beneath the contact zone upon repeated indentations at a constant P_{max}. Most phase changes take place in the first few cycles. The structure of the stress-induced new phases become stable and the response of the material will be completely elastic.

The load–displacement curves with the maximum load of 50 mN are presented in Fig. 1(b). The pop-out appears in the first indentation cycle, reflecting, as in the case of a Berkovich indenter, the formation of high-pressure crystalline phases in the transformation zone.[8] The maximum penetration depth in the second indentation cycle decreased substantially, indicating that the material in the transformed zone has less material still exhibiting hysteretic behavior. Pop-in is not so obvious on the loading part of the curve, occurring at a much higher load of 35 mN. Slopes of the very upper parts of the loading and unloading curves in the first and second cycles are nearly identical, with the values of 0.02 mN/nm on loading and 0.356 mN/nm on unloading. This may indicate that some further transformations occur when the load exceeds the pop-in load in the second cycle and the same type of decomposition on unloading before the pop-out event. The subsequent indentation cycles become almost identical. Similar to the first set of tests with $P_{max}=30$ mN, the response of the material is nearly elastic but the effective Young's modulus becomes higher (140 GPa) than that of the original diamond structure (137 GPa). Again, this gradual change of the indentation curves suggests that the structural change in the transformation zone takes place in the first few cycles. However, in the present case of $P_{max}=50$ mN, the stabilization process to the final elastic behavior was much accelerated if compared with the case of $P_{max}=30$ mN.

For the indentations under $P_{max}=90$ mN, the first cycle presents an obvious pop out on unloading. This was considered the result of the second phase transformation from β-Sn to SI-XII/SI-III.[2,5] The conclusion is reconfirmed here by Raman spectrum (Fig. 3, curve a) that shows the formation of the high-pressure phases Si-XII and Si-III in the first indentation cycle. Similarly, in the second indentation cycle, the slope of the loading curve substantially increases. Recalling the specification indicated by the Raman spectrum just discussed, it is easy to understand that this is partly due to the

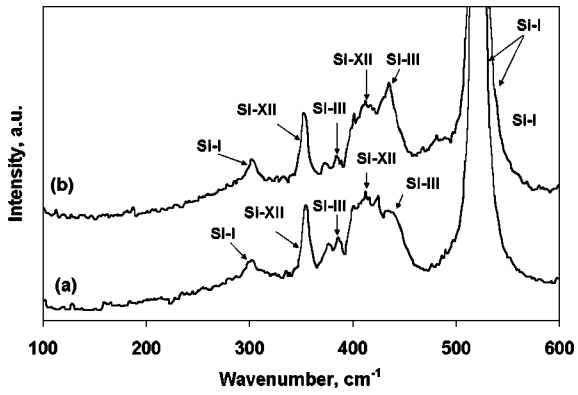

FIG. 3. Raman spectra from the samples after indentation with P_{max} =90 mN: (a) after the first cycle and (b) after the fifth cycle.

penetration of the indenter into the high-pressure phases, Si-XII and Si-III, that have different properties. The upper part of the loading curve beyond 80 mN deviates from elastic behavior and has a slope equal to that of the corresponding part in the first cycle, resembling the second cycle in the indentations with P_{max}=50 mN. The third to fifth indentation cycles indicate almost elastic and nonhysteresis behavior. The effective Young's modulus of the modified structure increases to 141 GPa. The phase composition of the transformation zone after the fifth indentation cycle, as presented in Fig. 3, curve b, shows a number of bands arising from phases Si-XII and Si-III.

If a material undergoes classical plastic deformation, the material in the later indentation cycles would follow the unloading path of the first cycle and possess a nonhysteresis behavior when P_{max} is a constant. This is certainly not the case in silicon under all the P_{max} studied. The deformation reached the nonhysteresis behavior only after some cycles of repeated indentations and the number of the cycles required depended on the values of P_{max}. With P_{max}=30 mN, such a transition needs four cycles. However, only three cycles were required when P_{max} is beyond 50 mN. This seems to indicate that in the first few cycles of repeated indentations under the same P_{max}, phase transformations take place until the material properties in the deformed zone become stable. The dependence of the transition upon the level of P_{max} seems to indicate that the rate of the phase change, which occurs during the transition upon unloading, is volume and stress dependent.

The force–displacement response of the phases induced by different P_{max} after multiple cycles are almost elastic (Fig. 2), though their effective Young's moduli are different (increased with the rise of P_{max}). This is not surprising upon recalling the previous studies under a single indentation at loads above the pop-in value, which reported that the structure of the transformation zone is highly dependent on P_{max}.[1] A low P_{max} promotes amorphous transformation but a greater P_{max} activates crystalline phases. On the other hand, Bradby *et al.*[5] found that the loading/unloading rate influences the formation of amorphous or crystalline phases. In the current case under repeated indentations, the structures developed in the first cycle at a given P_{max} will certainly alter the mechanical response in the second cycle. What is different here is the further evolution of the load–displacement curves from the second indentation cycle. This implies that indentations under the same P_{max} will also introduce phase changes. In addition, the results show that under the same P_{max}, phase transformations and material property stabilization take place within the first few cycles of repeated indentations. However, the transition of the load–displacement curves under different P_{max} indicates that the rate of the phase change is stress dependent.

At the fifth cycle, the response becomes nearly elastic (Fig. 2). Thus, no further phase transformation occurs. This is different from the result when silicon is loaded in a diamond anvil cell, where multiple loading–unloading cycles will initiate the diamond to β-Sn transformation[18] and the SIXII/SI-III phases were unstable and reversible.[14] The main difference between the loading by an anvil diamond cell and an indentation is that significant shear stresses appear in the latter. Although it has been proposed that the level of the deviatoric stress plays an important role in the phase changes in silicon,[2] it is unclear how a cyclic change of the stresses locks in the phase transformations and makes the high-pressure phases behave in an elastic manner.

In summary, this study identified some special properties of monocrystalline silicon when subjected to a cyclic microindentation. Different structures grew under different P_{max}. The response becomes elastic after a number of repeated indentations and a higher P_{max} hastened this property stabilization. In addition, the structures formed at different P_{max} have slightly different mechanical properties (effective Young's moduli in the present study). The transformed structure developed in the first indentation cycle is highly unstable and can be easily altered by a number of indentation variables. However, the detailed structural changes during the repeated indentations and the mechanisms of the property stabilization are still open questions.

[1] I. Zarudi and L. C. Zhang, Tribol. Int. **32**, 701 (1999).
[2] L. C. Zhang and I. Zarudi, Int. J. Mech. Sci. **43**, 1985 (2001).
[3] W. C. D. Cheong and L. C. Zhang, Nanotechnology **11**, 173 (2000).
[4] W. C. D. Cheong and L. C. Zhang, J. Mater. Sci. Lett. **19**, 439 (2000).
[5] J. E. Bradby, J. S. Williams, M. V. Wong-Leung, M. V. Swain, and P. Munroe, J. Mater. Res. **16**, 1500 (2001).
[6] L. C. Zhang and H. Tanaka, JSME Int. J., Ser. A **14**, 546 (1999).
[7] A. B. Mann, D. v. Heerden, J. B. Pethica, and T. P. Weihs, J. Mater. Res. **15**, 1754 (2000).
[8] V. Domnich, Y. G. Gogotsi, and S. N. Dub, Appl. Phys. Lett. **76**, 2214 (2000).
[9] Y. Q. Wu, X. Y. Yang, and Y. B. Xu, Acta Mater. **47**, 2431 (1999).
[10] D. R. Clarke, M. C. Kroll, P. D. Kirchner, and R. F. Cook, Phys. Rev. Lett. **60**, 2156 (1988).
[11] D. L. Callagan and J. C. Morris, J. Mater. Res. **7**, 1614 (1992).
[12] A. Keiler, Y. G. Gogotsi, and K. G. Nickel, J. Appl. Phys. **81**, 3057 (1997).
[13] K. Mizushima, S. Yip, and E. Kaxiras, Phys. Rev. B **50**, 14952 (1994).
[14] J. Crain, G. J. Ackland, J. R. Maclean, R. O. Piltz, P. D. Hatton, and G. S. Pawley, Phys. Rev. B **50**, 13043 (1994).
[15] A. Mujica, S. Radescu, A. Munoz, and R. J. Needs, Phys. Status Solidi B **223**, 379 (2001).
[16] G. M. Pharr, W. C. Oliver, and D. R. Clarke, J. Electron. Mater. **19**, 881 (1990).
[17] K. L. Johnson, *Contact Mechanics* (Cambridge, University Press, Cambridge, UK, 1985).
[18] R. O. Piltz, S. J. Macleans, S. J. Clark, G. L. Ackland, P. D. Hatton, and J. Crain, Phys. Rev. B **52**, 4072 (1995).